

Research on buffer structure and flow field simulation of swash plate plunger type hydraulic transformer^①

WANG Xiaojing (王晓晶)^{②*}, HUO Shuhang^{***}, LI Wenjie^{***}

(* Beijing Key Laboratory of Performance Guarantee on Urban Rail Transit Vehicle, Beijing University of Civil Engineering and Architecture, Beijing 102616, P. R. China)

(** Beijing Engineering Research Center of Monitoring for Construction Safety, Beijing University of Civil Engineering and Architecture, Beijing 102616, P. R. China)

(*** School of Mechanical and Power Engineering, Harbin University of Science and Technology, Harbin 150080, P. R. China)

Abstract

In order to solve the problem of excessive noise and vibration during the operation of the hydraulic transformer, an optimization method of valve plate damping hole structure is proposed to alleviate the phenomenon of pressure shock. Firstly, the mathematical model of oil pressure gradient in the plunger cavity is established, and the incremental equation of pressure change is derived. Secondly, a kind of buffering structure is proposed, the corresponding relationship between the pressure change and the envelopment angle of the buffering hole and the aperture size is determined by analyzing the oil pressure change curve in the plunger cavity. Finally, the flow field models with buffering holes are established, and the transient simulation of the pressure change process under the optimal solution is carried out with ANSYS software and the flow field pressure distribution contours are obtained. Through the analysis of simulation results, it is concluded that the optimal envelope angle of the three buffer holes of *A-T-B-A* is 5° , and the optimal aperture is 1.8 mm, 1.6 mm, and 1.7 mm, respectively. The buffer hole can achieve a better-buffering effect in the range of variable pressure angle $[0^\circ, 101^\circ]$. The buffer hole structure can effectively alleviate the pressure shock and reduce the noise level, which lays a foundation for the design and theoretical research of hydraulic transformers.

Key words: hydraulic transformer, pressure shock, buffer structure, flow field simulation, dynamic grid

0 Introduction

The secondary regulation system of the constant pressure network improves the system efficiency of hydraulic transmission. As the key component of the system, the hydraulic transformer can realize the non-destructive transmission of hydraulic energy with low cost, stable operation, and good control performance. However, due to the plunger structure of the hydraulic transformer, pressure pulsation and shock inside the plunger chamber are the main causes of noise and vibration of the system^[1-3]. Reducing pressure shock and flow fluctuation by optimizing the plunger distribution mechanism is one of the main methods to reduce noise and improve operation stability, and it is also a hot research topic in the field of hydraulic system^[4-5].

Over the years, domestic and foreign scholars have done a lot of research to improve the buffer performance of the distribution mechanism and promoted the further development and improvement of the new hydraulic transformer. The research on the buffer structure is mainly focused on the damping hole, triangular groove and composite structure form.

Xu et al.^[6] established a dynamic model of pulsation output by studying the fault supporting role and pressure relief groove of the flow valve mechanism, and proposed a simulation model optimization method to reduce the instantaneous flow. In order to improve the flow pulsation rate in the outlet, Hong et al.^[7] proposed a method based on numerical analysis to optimize the depth and width of the U-shaped buffer groove on the valve plate. Shentu et al.^[8] found that the port area was the main factor affecting the pressure impact

① Supported by the National Natural Science Foundation of China (No. 51975164) and Outstanding Youth of Pyramid Talent Training Project of Beijing University of Civil Engineering and Architecture (No. GDRC20220801).

② To whom correspondence should be addressed. E-mail: hitwangxiaojing@163.com.

Received on July 24, 2021

characteristics when studying the axial plunger structural elements, and pointed out that the outlet pulsation rate could be reduced by improving the cross-sectional area of the valve plate. Yang and Jiang^[9] developed a variable hydraulic transformer and proposed a compound buffer structure optimization scheme with self-adaptability of oil volume in the plunger chamber to suppress the port noise. Wang et al.^[10] used the computational fluid dynamics method to conduct dynamic simulation of the oil suction and discharge process of the piston pump, so as to establish a parameterized model for the valve plate structure and realize the optimization of triangular groove parameters.

In recent years, the research on the buffer structure of the new hydraulic transformer is mainly focused on the buffer groove structure, but there is little research on the influence of the buffer hole structure on noise and vibration. In this paper, the buffer hole structure is established on the valve plate to alleviate the pressure impact of the inclined plate plunger hydraulic transformer and further improve the stability of the inclined plate plunger hydraulic transformer.

1 Plunger cavity oil pressure gradient and its increment equation

During the operation of the inclined plate plunger hydraulic transformer, the oil volume in the plunger cavity changes. As shown in Fig. 1, a plunger is randomly selected as the research object, and the oil pressure gradient in the plunger cavity is deduced by the control volume method. It can be obtained according to the law of conservation of mass.

$$-\rho(q_{cv} + q_{cp} + q_{sp}) + \frac{d(\rho V_1)}{dt} + \frac{d(\rho V_2)}{dt} = 0 \quad (1)$$

where, q_{cv} is the oil leakage flow at the distribution pair (m^3/s), q_{cp} is the oil leakage flow at the plunger pair (m^3/s), q_{sp} is the oil leakage flow at the slipper pair (m^3/s), V_1 is the volume change caused by the movement of the plunger itself (m^3), V_2 is the volume change caused by the plunger suction or discharge of

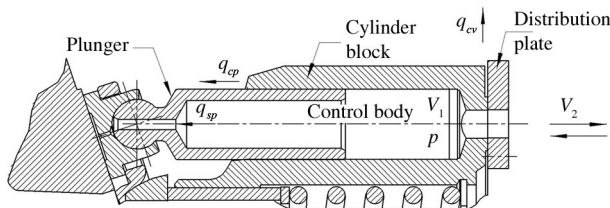


Fig. 1 The structure of plunger

oil from the distribution groove (m^3). ρ is the oil density (kg/m^3), and the oil density of No. 32 anti-wear hydraulic oil is $870 \text{ kg}/\text{m}^3$.

Due to the high volumetric efficiency and low leakage of the plunger element, after ignoring the leakage q_{cv} , q_{cp} , and q_{sp} , only the influence of the plunger movement and the connection between the plunger and the buffer structure is considered, and the oil pressure gradient in the plunger cavity with respect to angle φ ($^\circ$) can be obtained by

$$\frac{dp}{d\varphi} = - \frac{\beta_e \left(S_A R \tan \beta \sin(\varphi_0 + \varphi) \pm \frac{C_q \sqrt{2|\Delta p|/\rho} S_0}{6n} \right)}{V_{\min} + S_A R \tan \beta (1 - \cos \varphi_0)} \quad (2)$$

where, p is the pressure of oil in the plunger cavity (Pa); β_e is the elastic modulus of oil (Pa), and $\beta_e = 7 \times 10^8 \text{ Pa}$; V_{\min} is the minimum volume of oil in the plunger chamber (m^3), $V_{\min} = 6.22 \times 10^{-6} \text{ m}^3$; S_A is the plunger area (m^2), $S_A = 2.27 \times 10^{-4} \text{ m}^2$; R is the radius of the plunger distribution circle (m), $R = 0.0335 \text{ m}$; β is the swash plate angle ($^\circ$), $\beta = 18^\circ$. φ_0 is the angle from the bottom dead point of the plunger to the initial position of pre-lift/step-down ($^\circ$); C_q is the flow coefficient of the buffer structure, $C_q = 0.72$; Δp is the oil pressure difference between two adjacent grooves (Pa); n is the speed of swashplate plunger type hydraulic transformer (r/min), $n = 1000 \text{ r/min}$; S_0 is the minimum cross-sectional area of the buffer structure (m^2).

The increment equation is derived from the pressure gradient of oil in the plunger cavity.

$$\Delta p = - \frac{\beta_e \left(S_A R \tan \beta (\cos(\varphi_0) - \cos(\varphi_0 + \varphi)) \pm \int_0^\varphi \frac{C_q \sqrt{2|\Delta p|/\rho} S_0 d\varphi}{6n} \right)}{V_{\min} + S_A R \tan \beta (1 - \cos \varphi_0)} \quad (3)$$

Further,

$$\begin{cases} \Delta p_1 = - \frac{\beta_e S_A R \tan \beta (\cos(\varphi_0) - \cos(\varphi_0 + \varphi))}{V_{\min} + S_A R \tan \beta (1 - \cos \varphi_0)} \\ \Delta p_2 = \pm \frac{\beta_e \int_0^\varphi \frac{C_q \sqrt{2|\Delta p|/\rho} S_0 d\varphi}{6n}}{V_{\min} + S_A R \tan \beta (1 - \cos \varphi_0)} \end{cases} \quad (4)$$

where, Δp_1 is the change of oil pressure in the plunger cavity caused by the plunger movement (Pa), Δp_2 is the change of oil pressure in the plunger cavity caused by the buffer structure (Pa).

2 Optimal design of valve plate buffer structure

Envelope angle $\Delta\varphi$ of buffer structure of different

sizes is taken and substituted into Eq. (3) when φ_0 is in the interval of $[0^\circ, 120^\circ]$, and the change curves of oil pressure in the plunger cavity caused by the plunger movement are obtained, as shown in Fig. 2.

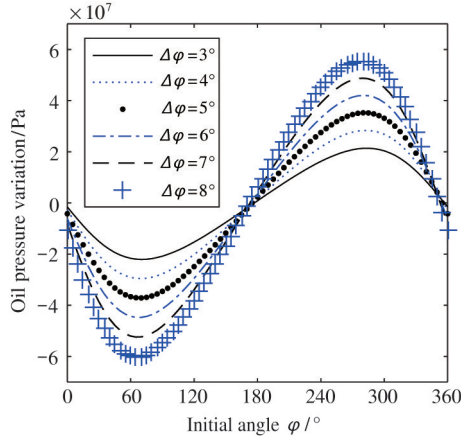


Fig. 2 Pressure curves caused by plunger motion

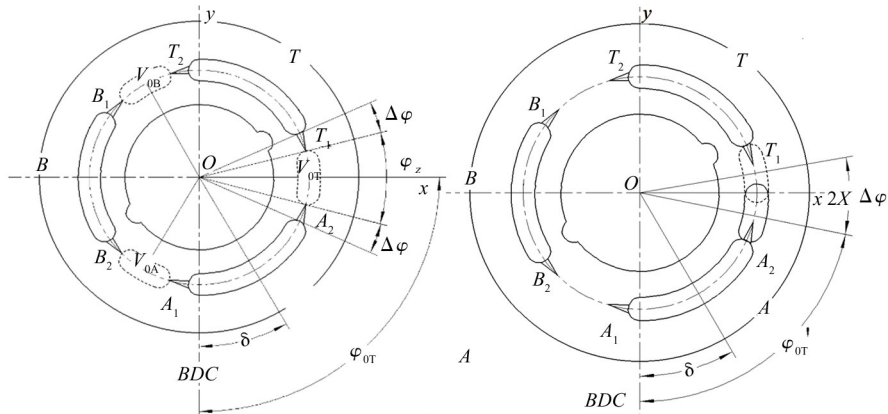


Fig. 3 Pressure curves caused by plunger motion

When the hydraulic transformer is in a balanced state, its speed is constant. From the law of conservation of energy, the power balance equation of hydraulic transformer can be obtained as follows.

$$p_A q_A + p_B q_B + p_T q_T - W_{loss} = 0 \quad (5)$$

In Eq. (5), p_A , p_B , and p_T are the pressure of the grooves A , B , T respectively (Pa); q_A , q_B , and q_T are the flow rate of the distribution groove A , B , T , respectively (m^3/s); W_{loss} is the power loss caused by viscous friction torque, sliding friction torque and leakage (kW)

In general, take W_{loss} as 0 kW, and the formula of variable pressure ratio about variable pressure angle can be obtained from Ref. [11].

$$\Pi = -\frac{q_A}{q_B} = -\left(\frac{\sin\delta}{\sin(240^\circ + \delta)} + \frac{\sin(120^\circ + \delta)p_T}{\sin(240^\circ + \delta)p_A}\right) \quad (6)$$

In Eq. (6) Π is the ratio of output and input

pressure. In the interval of $[0^\circ, 120^\circ]$, $|\Delta p_1|$ is less than the rated pressure of swashplate plunger type hydraulic transformer 40 MPa, so the buffer structure envelopment angle $\Delta\varphi$ is 5° . And the product of the maximum pressure variation ratio of the swashplate plunger type hydraulic transformer and the oil source pressure should not be greater than the rated pressure of 40 MPa. At present, the maximum voltage change ratio of the swashplate plunger hydraulic transformer is 1.2–4.8. For the insurance purpose, the maximum pressure change ratio is 4 : 1, and the pressure of the low-pressure groove is 0 MPa, then the pressure of the oil source is 8 MPa.

The triangular groove represents the position of the buffer structure, as shown in Fig. 3. In Fig. 3, δ is the pressure adjustment angle of the hydraulic transformer, which is defined as the angle between the center point of the xoy plane of the valve plate and the equal point of the groove A and the negative half-axis direction of the y axis.

pressure.

Take p_T as 0 MPa, and the following relation can be obtained.

$$\Pi = -\frac{q_A}{q_B} = -\frac{\sin\delta}{\sin(240^\circ + \delta)} \quad (7)$$

V_{OT} , V_{OB} , and V_{OA} are the oil volume in the plunger cavity respectively when the plunger is just in the middle position of groove $A-T$, groove $T-B$, and groove $B-A$. The magnitude of its angle relative to the lower dead point BDC is denoted as A , B and C respectively. At the same time, when the plunger is just out of the groove A , T , and B , the position of the plunger angle is φ_{OT}' , φ_{OB}' , and φ_{OA}' . The relationship is as follows.

$$\begin{cases} \varphi_{OT} = \delta + 60^\circ \\ \varphi_{OB} = \delta + 180^\circ \\ \varphi_{OA} = \delta - 60^\circ \end{cases}, \begin{cases} \varphi_{OT}' = \varphi_{OT} - \Delta\varphi \\ \varphi_{OB}' = \varphi_{OB} - \Delta\varphi \\ \varphi_{OA}' = \varphi_{OA} - \Delta\varphi \end{cases} \quad (8)$$

When the size of the Δp_2 is the same value, the pressure change caused by the buffer hole is more sta-

ble and uniform than the triangular groove, and the influence of Δp_1 can be better balanced in the global state. Therefore, the stage of changing the cross-sectional area of the overcurrent with shorter buffer hole is ignored, and the buffer hole structure is used for design and analysis.

$$S_0 = \frac{\pi d^2}{4} \quad (9)$$

where, d is the diameter of the buffer hole (m).

When the plunger runs between the distribution windows, the pressure change Δp_2 can be divided into Δp_{21} and Δp_{22} when it passes through two buffer structures, and then $\Delta p_2 = \Delta p_{21} + \Delta p_{22}$.

$$\begin{cases} \Delta p_{21} = \frac{\pm \frac{\beta_e \Delta \varphi C_q \pi d^2}{24n} \sqrt{\frac{|\Delta p|}{\rho}}}{V_{\min} + S_A R \tan \beta (1 - \cos(\varphi_{01}'))} \\ \Delta p_{22} = \frac{\pm \frac{\beta_e \Delta \varphi C_q \pi d^2}{24n} \sqrt{\frac{|\Delta p|}{\rho}}}{V_{\min} + S_A R \tan \beta (1 - \cos(\varphi_{01}))} \end{cases} \quad (10)$$

The plus or minus sign of Δp_2 depends on the over-step-down or over-boost caused by Δp_1 . In order to alleviate the pressure impact inside the hydraulic transformer, Δp_1 and Δp_2 need to cooperate with B to complete the pre-step-up/step-down process ahead of time.

In summary, when the oil source pressure is 8 MPa, the pressure of the low-pressure groove T is 0 MPa, the envelope angle of the buffer hole $\Delta \varphi$ is 5° , and the variable pressure angle is 101° , the maximum variable pressure ratio is 3 : 1, the optimal design of the buffer hole structure can be carried out under the above conditions.

2.1 Design of buffer structure in the pressure variation range of groove A-T

For the pre-depressurization range from groove A to groove T, there is $\Delta p_1 < 0$ and $\Delta p_2 > 0$. In order to enable Δp_2 to cooperate with Δp_1 to complete the pre-depressurization process ahead of time, Eq. (11) should be satisfied.

$$\begin{cases} \Delta p_1 + \Delta p_2 - \Delta p_{A-T} \geq 0 \\ \Delta p_{A-T} = p_T - p_A \end{cases} \quad (11)$$

Further,

$$\begin{aligned} & \frac{\frac{\beta_e \Delta \varphi C_q \pi d_{A-T}^2}{24n} \sqrt{\frac{|\Delta p_{A-T}|}{\rho}}}{V_{\min} + S_A R \tan \beta (1 - \cos(\delta + 60^\circ - \Delta \varphi))} \\ & + \frac{\frac{\beta_e \Delta \varphi C_q \pi d_{A-T}^2}{24n} \sqrt{\frac{|\Delta p_{A-T}|}{\rho}}}{V_{\min} + S_A R \tan \beta (1 - \cos(\delta + 60^\circ))} \\ & - \frac{\beta_e S_A R \tan \beta (\cos(\delta + 60^\circ - \Delta \varphi) - \cos(\delta + 60^\circ + \Delta \varphi))}{V_{\min} + S_A R \tan \beta (1 - \cos(\delta + 60^\circ - \Delta \varphi))} \\ & - \Delta p_{A-T} \geq 0 \end{aligned} \quad (12)$$

When the diameter of buffer hole is 1.5 mm, 1.6 mm, 1.7 mm, 1.8 mm, 1.9 mm and 2.0 mm, the buffering effect curves are shown in Fig. 4.

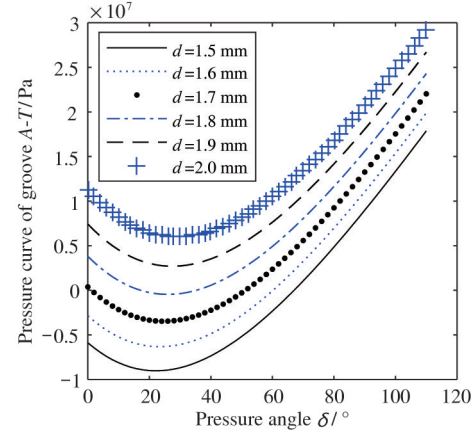


Fig. 4 Comparison of buffering effect curves of different buffer holes in groove A-T

As can be seen from Fig. 4, when the diameter of the buffer hole is 1.8 mm, Eq. (12) can be satisfied. Because the excessive diameter of the buffer hole will affect the error, which is ignored when the buffer hole is regarded as a constant cross-sectional area buffer structure. The buffer hole A_2 and T_1 in the pre-pressure range from groove A to T should be as small as possible. Thus, the diameter should be taken as 1.8 mm.

2.2 Design of buffer structure in the pressure variation range of groove T-B

For the pre-depressurization range from groove A to groove T, there is $\Delta p_1 > 0$ and $\Delta p_2 < 0$. In order to enable Δp_2 to cooperate with Δp_1 to complete the pre-boost process ahead of time, Eq. (13) should be satisfied.

$$\begin{cases} \Delta p_{T-B} = p_A \frac{-\sin(\delta)}{\sin(240^\circ + \delta)} - p_T \\ \Delta p_1 + \Delta p_2 - \Delta p_{T-B} \leq 0 \end{cases} \quad (13)$$

Further,

$$\begin{aligned} & \frac{\frac{\beta_e \Delta \varphi C_q \pi d_{T-B}^2}{24n} \sqrt{\frac{|\Delta p_{T-B}|}{\rho}}}{V_{\min} + S_A R \tan \beta (1 - \cos(\delta + 180^\circ - \Delta \varphi))} \\ & - \frac{\frac{\beta_e \Delta \varphi C_q \pi d_{T-B}^2}{24n} \sqrt{\frac{|\Delta p_{T-B}|}{\rho}}}{V_{\min} + S_A R \tan \beta (1 - \cos(\delta + 180^\circ))} \\ & - \frac{\beta_e S_A R \tan \beta (\cos(\delta + 180^\circ - \Delta \varphi) - \cos(\delta - 180^\circ - \Delta \varphi))}{V_{\min} + S_A R \tan \beta (1 - \cos(\delta + 180^\circ - \Delta \varphi))} \\ & - \Delta p_{T-B} \leq 0 \end{aligned} \quad (14)$$

When the diameter of buffer hole is 1.5 mm, 1.6 mm, 1.7 mm, 1.8 mm, 1.9 mm and 2.0 mm, the buffering effect curves are shown in Fig. 5.

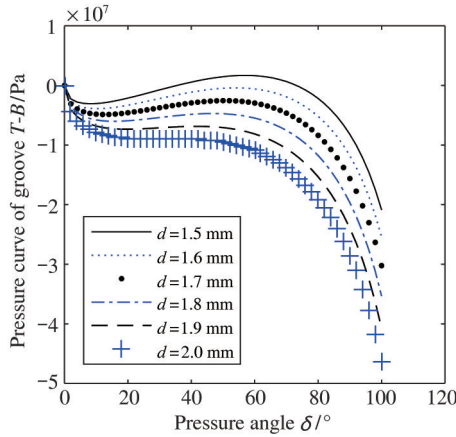


Fig. 5 Comparison of buffering effect curves of different buffer holes in groove $T-B$

As can be seen from the figure, when the diameter of the buffer hole is 1.6 mm, the Eq. (14) can be satisfied. For the reasons in subsection 3.1, the diameter of the buffer hole T_2 and B_1 in the pre-boosting area from the groove T to B is 1.6 mm.

2.3 Design of buffer structure in the pressure variation range of groove $B-A$

In the range of variable pressure angle $[0^\circ, 60^\circ]$, there is a pre-boost range from groove B to A , $\Delta p_1 > 0$ and $\Delta p_2 < 0$. In order to enable Δp_2 to cooperate with Δp_1 to complete the pre-boosting process ahead of time, Eq. (15) should be satisfied.

$$\begin{cases} \Delta p_{B-A} = p_A - p_A \frac{-\sin(\delta)}{\sin(240^\circ + \delta)} \\ \Delta p_1 + \Delta p_2 - \Delta p_{B-A} \leq 0 \end{cases} \quad (15)$$

Further,

$$\begin{aligned} & -\frac{\beta_e \Delta \varphi C_q \pi d_{B-A}^2}{24n} \sqrt{\frac{|\Delta p_{B-A}|}{\rho}} \\ & \frac{V_{\min} + S_A R \tan \beta (1 - \cos(\delta - 60^\circ - \Delta \varphi))}{V_{\min} + S_A R \tan \beta (1 - \cos(\delta - 60^\circ))} \\ & - \frac{\beta_e \Delta \varphi C_q \pi d_{B-A}^2}{24n} \sqrt{\frac{|\Delta p_{B-A}|}{\rho}} \\ & - \frac{S_A R \tan \beta (\cos(\delta - 60^\circ - \Delta \varphi) - \cos(\delta - 60^\circ + \Delta \varphi))}{V_{\min} + S_A R \tan \beta (1 - \cos(\delta - 60^\circ - \Delta \varphi))} \\ & - \Delta p_{B-A} \leq 0 \end{aligned} \quad (16)$$

When the diameter of buffer hole is 1.5 mm, 1.6 mm, 1.7 mm, 1.8 mm, 1.9 mm and 2.0 mm, the buffering effect curves are shown in Fig. 6.

As can be seen from the figure, when the diameter of the buffer hole is 1.7 mm, Eq. (16) can be satisfied. For the reasons in subsection 2.1, the diameter of buffer holes B_2 and A_1 is 1.7 mm in the pressure variation angle range $[0^\circ, 60^\circ]$, when the groove B to A is the pre-step-down interval.

In the variable pressure range $[60^\circ, 101^\circ]$, there is a

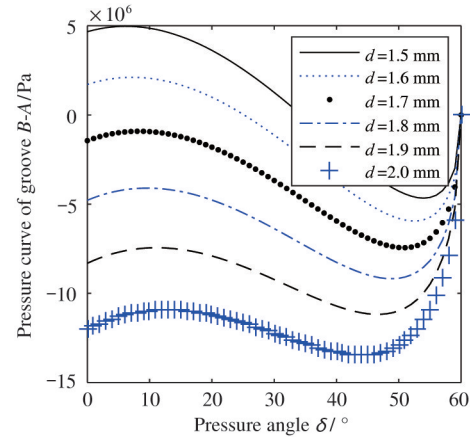


Fig. 6 Comparison of buffering effect curves of different buffer holes in groove $B-A [0^\circ, 60^\circ]$

pre-depressurization zone from groove B to A , $\Delta p_1 < 0$, $\Delta p_2 > 0$. In order to enable Δp_2 to cooperate with Δp_1 to complete the pre-depressurization process ahead of time, the following relationship is established.

$$\begin{cases} \Delta p_{B-A} = p_A - p_A \frac{-\sin(\delta)}{\sin(240^\circ + \delta)} \\ \Delta p_1 + \Delta p_2 - \Delta p_{B-A} \geq 0 \end{cases} \quad (17)$$

Further,

$$\begin{aligned} & -\frac{\beta_e \Delta \varphi C_q \pi d_{B-A}^2}{24n} \sqrt{\frac{|\Delta p_{B-A}|}{\rho}} \\ & \frac{V_{\min} + S_A R \tan \beta (1 - \cos(\delta - 60^\circ - \Delta \varphi))}{V_{\min} + S_A R \tan \beta (1 - \cos(\delta - 60^\circ))} \\ & - \frac{\beta_e \Delta \varphi C_q \pi d_{B-A}^2}{24n} \sqrt{\frac{|\Delta p_{B-A}|}{\rho}} \\ & - \frac{S_A R \tan \beta (\cos(\delta - 60^\circ - \Delta \varphi) - \cos(\delta - 60^\circ + \Delta \varphi))}{V_{\min} + S_A R \tan \beta (1 - \cos(\delta - 60^\circ - \Delta \varphi))} \\ & - \Delta p_{B-A} \geq 0 \end{aligned} \quad (18)$$

When the diameter of buffer hole is 1.0 mm, 1.1 mm, 1.2 mm, 1.3 mm, 1.4 mm and 1.5 mm, the curves are shown in Fig. 7.

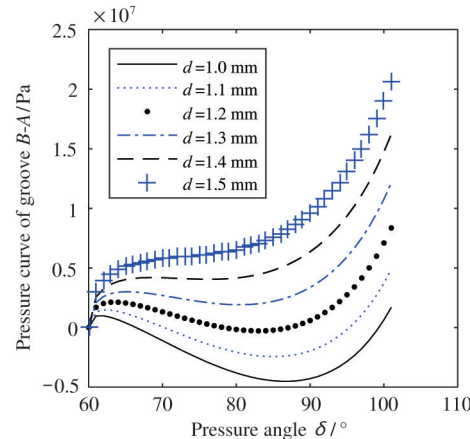


Fig. 7 Comparison of buffering effect curves of different buffer holes in groove $B-A [60^\circ, 101^\circ]$

As can be seen from Fig. 7, when the diameter of the buffer hole is 1.2 mm, Eq. (18) can be satisfied. For the reasons in subsection 2. 2, the diameter of buffer holes B_2 and A_1 is 1.2 mm in the pressure variation angle range $[60^\circ, 101^\circ]$, when the groove B to A is the pre-step-down interval.

Considering the overall situation, in order to complete the pre-step-up/step-down process ahead of time, the diameters of buffer holes B_2 and A_1 should be 1.7 mm in the range of variable pressure angle $[0^\circ, 101^\circ]$.

3 Simulation analysis of flow field

In order to avoid the closed dead volume of the

hydraulic transformer in the working process, the angle of temporarily connecting the two distribution grooves through the buffer structure is 1° , that is, the angle between the actual grooves is 9° . On this basis, the simulation study of inclined plate plunger hydraulic transformer is carried out when the variable voltage angle is $30^\circ, 60^\circ, 90^\circ$ and 101° respectively. When the variable pressure angle is 30° , the groove $B-A$ is in the pre-boost range, and the transformer ratio is $2:1$, the input pressure p_A is 8 MPa, and the output pressure p_B is 4 MPa, and the pressure cloud diagram is shown in Fig. 8.

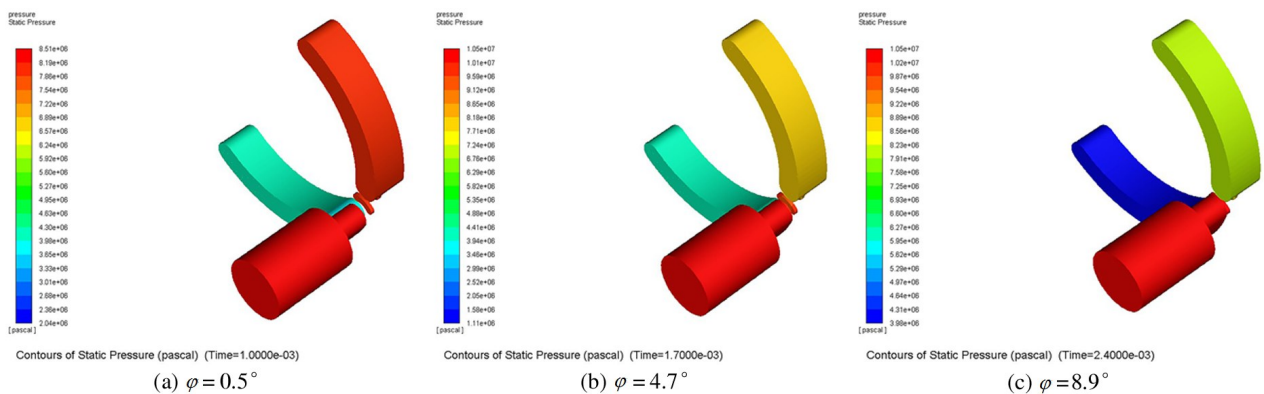


Fig. 8 Piston pressure cloud diagram when $\delta = 30^\circ$

When the pressure change angle is 30° , the average mass pressure curve of the oil in the plunger cavity in the pre-boost interval of groove $B-A$ is shown in Fig. 9.

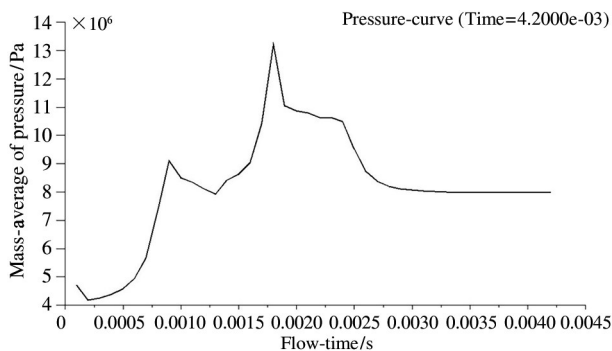


Fig. 9 Mass-average pressure curve of oil in piston cavity when $\delta = 30^\circ$

As can be seen from Fig. 9, when $t < 0.0001$ s, the oil pressure in the plunger cavity is already increasing when it leaves groove B . When $t = 0.0017$ s, the plunger is about to leave the buffer hole B_2 and contact the buffer hole A_1 , and the oil pressure in the plunger cavity rises steeper, and then the pressure drops under the influence of buffer hole A_1 and remains within a

certain range. When $t > 0.0024$ s, the plunger contacts groove A , and the oil pressure in the plunger cavity quickly matches to the pressure value of groove A .

When the pressure change angle is 60° , the pressure of groove B is the same as that of groove A . At this time, the pressure change ratio is $1:1$, the input pressure p_A is 8 MPa, and the output pressure p_B is 8 MPa, and the pressure cloud diagram is shown in Fig. 10.

When the pressure variation angle is 60° , the average mass pressure curve of the oil in the plunger cavity in the $B-A$ pressure variation interval of the groove is shown in Fig. 11.

As can be seen from Fig. 11, at this time, the average mass pressure of oil in the plunger cavity continues to be within the range of 7.9 MPa – 8.25 MPa, which can be regarded as the expected buffering effect of buffering hole B_2 and buffering hole A_1 .

When the pressure change angle is 90° , groove $B-A$ is the pre-step-down interval, and the pressure change ratio is $1:2$, the input pressure p_A is 8 MPa, and the output pressure p_B is 16 MPa, and the pressure cloud diagram is shown in Fig. 12.

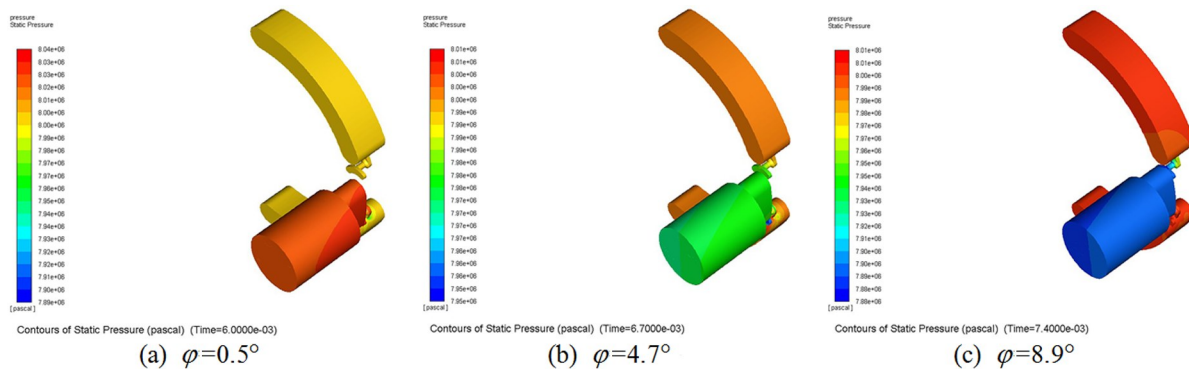


Fig. 10 Piston pressure cloud diagram when $\delta = 60^\circ$

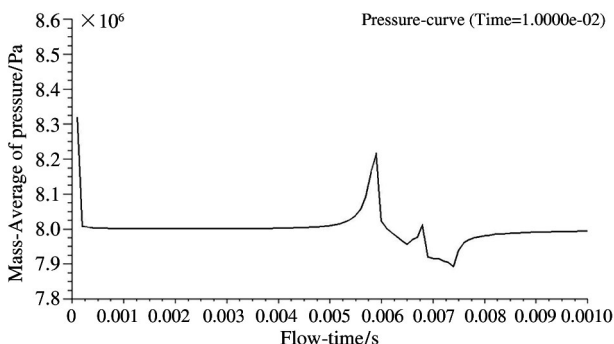


Fig. 11 Mass-average pressure curve of oil in piston cavity when $\delta = 60^\circ$

When the pressure variation angle is 90° , the average mass pressure curve of oil in the plunger cavity in the pre-depressor interval of groove $B-A$ is shown in Fig. 13.

As can be seen from Fig. 13, when $t < 0.0043$ s, the oil pressure in the plunger cavity is already depressurizing when it leaves groove B . When $t = 0.005$ s, the plunger is about to break away from the buffer hole B_2 and contact the buffer hole A_1 , and the oil pressure in the plunger cavity drops sharply, and then remains within a certain range under the action of the buffer

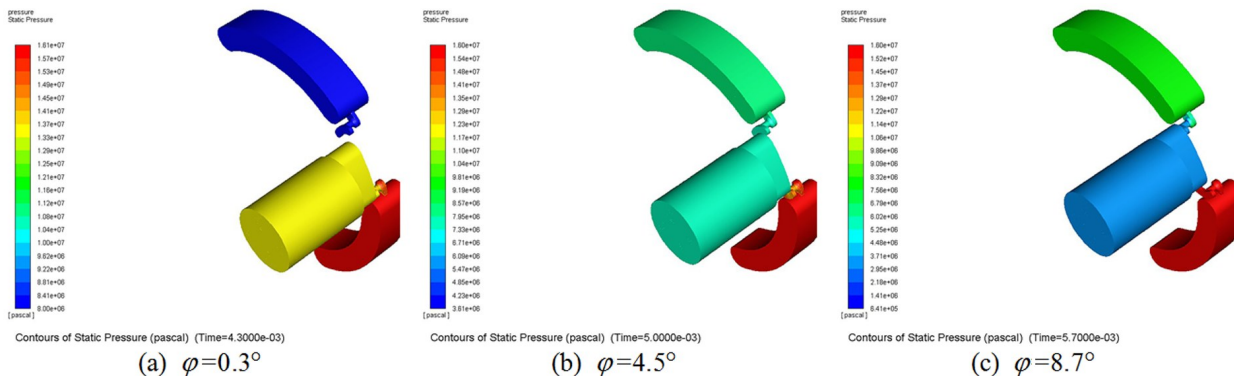


Fig. 12 Piston pressure cloud diagram when $\delta = 90^\circ$

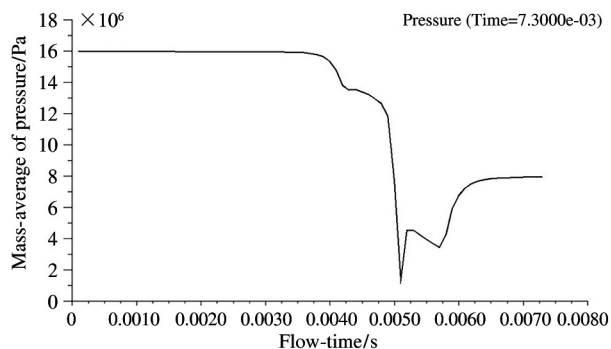


Fig. 13 Mass-average pressure curve of oil in piston cavity when $\delta = 90^\circ$

hole A_1 . The fluctuation in the Fig. 13 is due to the fact there is a certain low-pressure area in part of the interval at this stage, which affects the value of the average mass pressure of the oil in the plunger cavity. When $t > 0.0057$ s, the plunger contacts groove A , and the oil pressure in the plunger cavity quickly matches to the pressure value of groove A .

When the pressure change angle is 101° , groove $B-A$ is the pre-step-down interval, and the pressure change ratio is 1 : 3, the input pressure p_A is 8 MPa, and the output pressure p_B is 24 MPa, and the pressure cloud diagram is shown in Fig. 14.

When the pressure variation angle is 101° , the average mass pressure curve of oil in the plunger cavity in the pre-depressurizing interval of groove $B-A$ is shown in Fig. 15.

As can be seen from Fig. 15, when $t < 0.0061$ s, the oil pressure in the plunger cavity is already depressurizing when it leaves groove B . When $t = 0.0069$ s, the

plunger is about to break away from the buffer hole B_2 and contact the buffer hole A_1 , the oil pressure in the plunger cavity drops sharply, and then remains within a certain range under the action of the buffer hole A_1 . In this process, the movement of the plunger causes a great negative pressure area, which affects the value of

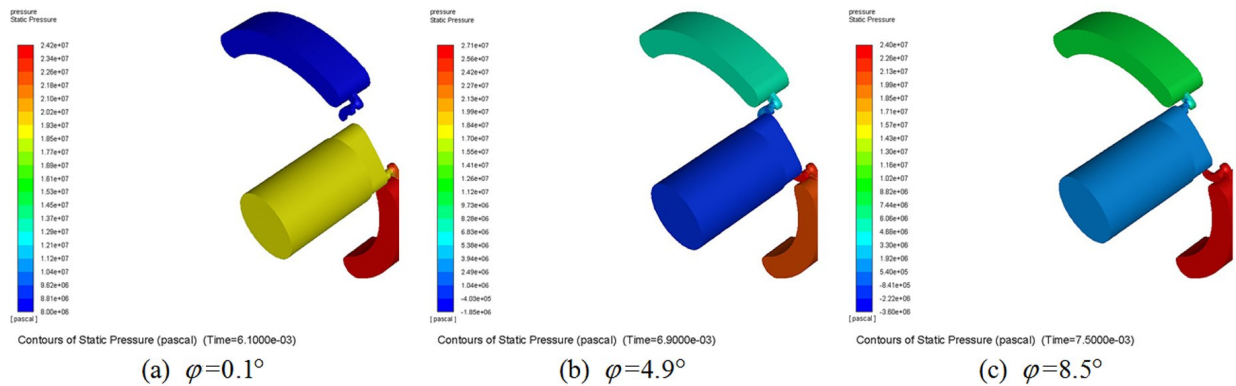


Fig. 14 Piston pressure cloud diagram when $\delta = 101^\circ$

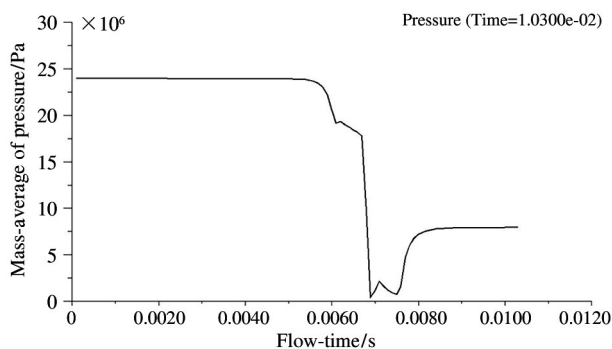


Fig. 15 Mass-average pressure curve of oil in piston cavity when $\delta = 90^\circ$

the average force of the mass of the plunger, and the feedback becomes a fluctuation phenomenon of sudden pressure drop in the figure. When $t > 0.0075$ s, the plunger contacts groove A , and the oil pressure in the plunger cavity quickly matches to the pressure value of groove A .

4 Conclusions

A buffer hole structure of inclined plate plunger hydraulic transformer is proposed. It is calculated that the optimal envelope angle of the three buffer holes of $A-T-B-A$ is 5° , and the optimal dimension is 1.8 mm, 1.6 mm and 1.7 mm respectively. The transient process of the pressure change of the plunger during the transition between different grooves is simulated, and the

cloud diagram of the flow field and pressure distribution in the high-speed operation of the hydraulic transformer is obtained. The simulation results show that the buffer structure can achieve better buffering effect in the range of variable pressure angle $[0^\circ, 101^\circ]$. At the same time, through the analysis of the simulation results, it is concluded that the amplitude of pressure change increases with the increasing of the transformer ratio of the hydraulic transformer.

References

- [1] XIAO H, XIE R, WAN Y. Energy-saving technological progress and the construction of two-oriented society in Hunan Province [J]. *Progress and Countermeasures of Science and Technology*, 2012, 29 (9) : 36-421
- [2] YANG D X, WANG C M, LIU X X, Energy saving and emission reduction of hydraulic system[J]. *Scientific and Technological Innovation and Application*, 2012, 3 (3) : 87-87
- [3] YANG H Y, OUYANG X P, XU B. Development status of hydraulic transformers[J]. *Journal of Mechanical Engineering*, 2003, 39(5) : 1-5
- [4] PAN Y, LI Y B, HUANG M H, et al. Optimization of valve plate and analysis of flow pulsation characteristics of dual-couplet axial piston pump [J]. *Transactions of the Chinese Society for Agricultural Machinery*, 2016, 47(4) : 391-398 (In Chinese)
- [5] LIU Y L, SHI W J, XU S. Analysis of characteristics of axial piston pump based on virtual prototyping technology [J]. *Modern Manufacturing Engineering*, 2016, 9:25-29
- [6] XU B, YE S G, ZHANG J H, et al. Flow ripple reduc-

- tion of an axial piston pump by a combination of cross-angle and pressure relief grooves: analysis and optimization [J]. *Journal of Mechanical Science and Technology*, 2016, 30(6):2531-2545
- [7] HONG H C, ZHANG B, YU M, et al. Analysis and optimization on U-shaped damping groove for flow ripple reduction of fixed displacement axial-piston pump[J]. *International Journal of Fluid Machinery and Systems*, 2020, 13(1):126-135
- [8] SHENTU S N, RUAN J, QIAN J Y, et al. 2D optimization analysis of pump flow characteristics and distribution window[J]. *Journal of Agricultural Machinery*, 2019, 50(12):403-410
- [9] YANG G Z, JIANG J H. Flow characteristics of variable hydraulic transformer[J]. *Journal of Central South University*, 2015, 22(6):2137-2148
- [10] WANG A L, WU X F, MM B, et al. Dynamic response relationship between plunger pump distribution structure and flow characteristics[J]. *Journal of Tongji University (Natural Science)*, 2011, 39(4):586-590(In Chinese)
- [11] JIANG J H, DU Z, SHEN W. Research on energy saving of linear actuator based on hydraulic transformer [J]. *Journal of East China University of Science and Technology*, 2020, 48(2):116-121 (In Chinese)

WANG Xiaojing, born in 1981. She received her Ph. D degree in School of Mechatronics Engineering of Harbin Institute of Technology in 2009. Her research interests include fluid transmission and control, optimum design of hydraulic components and novel hydraulic device.